Computer Vision for Detecting and Measuring Multicellular Tumor Shperoids of Prostate Cancer

Alex Wojaczek
School of Computing
Queen's University
Kingston, Canada
a.wojaczek@queensu.ca

Regina-Veronicka Kalaydina
Biomedical and Molecular Science
Queen's University
Kingston, Canada
nicka.kalaydina@queensu.ca

Mohammed Gasmallah
School of Computing
Queen's University
Kingston, Canada
11mhg@queensu.ca

Dr. Myron R. Szewczuk
Biomedical and Molecular Science
Queen's University
Kingston, Canada
szewczuk@queensu.ca

Dr. Farhana Zulkernine
School of Computing
Queen's University
Kingston, Canada
farhana@queensu.ca

***Abstract*—We present a deep learning model to apply computer vision to detect prostate cancer spheroid cultures and calculate their volume. Multicellular tumour spheroids, or simply spheroids, represent a three-dimensional in vitro model of cancer. Spheroids are being increasingly used in drug discovery due to their superior ability to mimic the tumor microenvironment compared to monolayer cell cultures. A reduction in spheroid size in response to treatment with anticancer agents is indicative of the success of the therapy. As such, accurate spheroid detection and volume estimation is critical in assays involving spheroids. Automating spheroid detection and measurement reduces manual labor, laboratory costs, and research time. Our system is implemented using Darkflow YOLOv2, a single-phase object detector, based on a twenty-four-layer convolutional neural network. The network is trained on the custom data of biochemically-generated spheroids and their corresponding images, which are then bound and detected with an F1-score of 76% and an IoU of 69%. Volume calculations applied to the identified spheroids resulted in a high volume estimation accuracy with only 3.99% average error.**

Keywords—convolutional neural networks, YOLOv2, spheroids, object detection, volumetric measurements

1 INTRODUCTION

Among the existing cancer models used at the preclinical stage, multicellular tumour spheroids (MCTS) are becoming increasingly popular [1]. In general, spheroids are "multicellular aggregates measuring up to 1mm in diameter obtained from single cells" [2]. Spheroids are a three-dimensional (3D) in vitro model of cancer used for the study tumor biology, toxicology, and evaluation of potential chemotherapeutics [3]. Volumes of spheroids before and after treatment with anticancer agents are challenging to estimate, but provide important information regarding the efficacy of the potential treatment [4]. Traditionally, manual identification and volume measurement of spheroids has been used to track spheroids growth kinetics in response to therapy. However, manual analysis is costly, time-consuming and prone to human error due to subjective and qualitative assumptions made by the laboratory personnel, who require time and training to properly identify and measure spheroids [5]. Automated spheroid detection and measurement systems can circumvent some of these issues, as computers can process the images of the spheroids and expedite the detection, measurement, and archival of the data. Some of the applications used to replace manual spheroid analysis include high-throughput functional assays, edge detection methods, machine learning (ML) approaches, and 3D volume reconstruction [6]. ML is an emerging area of research as it relates to spheroid analysis [7, 8]. As such, we propose a novel supervised ML approach to tackle the problem of spheroid detection and volume estimation.

1.1 MOTIVATION

Compared to monolayer or two-dimensional cell cultures, MCTS have been reported to recapitulate with better fidelity the organization of cells found in vivo [9]. Physiologically relevant preclinical modelling systems can reduce the high numbers of ineffective drugs that have proceeded into in vivo assays, which have negatively affected the overall length and cost of the drug discovery process [10]. Concerns have also been raised with respect to the overuse of animas in the drug discovery pipeline [11]. As such, MCTS are a practical alternative, serving as an intermediate solution between 2D monolayer cell cultures and animal models [9]. Automated systems allow for simple and standardized assays for spheroid image analysis, quantification, and automation for drug screening purposes [4].

Computer vision has enhanced the high-throughput potential of spheroids as a modelling system and improvements to spheroid analysis using machine learning are of particular research interest. Two key considerations include a high sensitivity to false positives and the ability to process multiple spheroids per image, serving as improvements to existing models [12]. Thus, we propose the You Only Look Once framework for detection and volume estimation of MCTS generated from prostate cancer cells using a biochemical technique.

1.2 KEY CONTRIBUTIONS

We propose a novel framework that applies computer vision and ML techniques to help alleviate the time and cost associated with the manual recognition, labelling and measurement of spheroids with a view to implement a standardized process across studies employing spheroids. We developed a framework for identification, classification, and volume estimation of spheroids using a deep convolutional neural network (CNN). We also demonstrate the efficacy of multiple types of preprocessing that can be applied to these images.

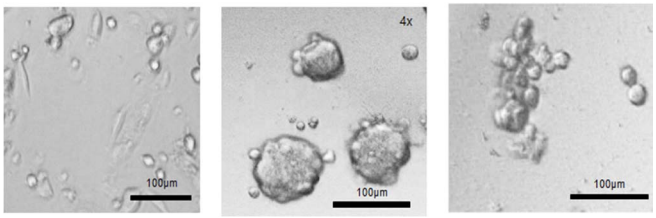

(a) monolayer cells **(b) 3D spheroids** **(c) cell aggregates**

Figure 1: DU145 prostate cancer cells, greyscale.

2 BACKGROUND

Multicellular tumor spheroids (MCTS) are a three-dimensional cell culture model that bridges the gap between two-dimensional cell culture and animal models. Generally, spheroids are defined as "spherically symmetric aggregates of cells analogous to tissues" [13] as outlined in Fig. 1. However, it is not uncommon for research laboratories to employ their own definitions of a spheroid, which contributes to the lack of standardization in spheroid analysis. For the purposes of this study, the following definition was used, as per the specifications of the laboratory of Dr. Myron R. Szewczuk: "compact rounded spheroids with a distinct border that has a diameter of at least 60 microns, and contain cells which are indistinguishable from one another" [14, 15]. Spheroids are capable of reproducing growth kinetics, oxygen, gases, nutrient and waste gradients, proliferate distribution, and gene expression profiles among other properties of small, solid avascular tumors [16]. The properties of the MCTS are highly dependent on their surface area and volume. Small spheroids having less than or equal to 150 µm diameter may exhibit 3D cell–cell and cell–matrix interactions, while spheroids with a diameter of 200 to 500 µm develop chemical gradients. Large spheroids of greater than 500 µm diameter establish central secondary necrosis [17, 18]. These properties make them useful in the study of cancer cell metabolism, tumor micro-environment signaling cross-talk, cancer stem cells, and drug screening [19].

The underlying theme among techniques that promote spheroid formation is the promotion of cell-cell interactions over cell-surface interactions [20]. To state briefly, techniques for spheroid generation include agitation-based methods, the hanging drop technique, the liquid overlay approach, non-adherent techniques, assembly/magnetic approaches, Bioprinting, 3D scaffolds, and the application of microfluids [21, 22]. Each of these methods has specific trade-offs regarding the need for specialized equipment, the ability to control the shape and size of spheroids, and the ease of drug screening performance [23, 24].

The spheroids used for this particular work are formed with a biochemical method using cyclic Arg-Gly-Asp-D-Phe-Lys peptide modified with 4-carboxybutyl-triphenylphosphonium bromide, or cyclo-RGDfK(TPP)) [25]. The RGD motif is present in the naturally-occurring protein, fibronectin, found in the ECM [26]. As such, cyclo-RGDfK (TPP)-mediated spheroid formation is thought to more accurately recapitulate the tumor micro-environment than other 3D models [25]. Spheroids generated from cyclo-RGDfK (TPP) can provide insights into cancer biology by emphasizing the importance of cell-cell adhesion interactions and simulating the tumor microenvironment. Our research focuses on automating the identification and measurement of the spheroids which are fundamental to studies involving spheroids.

In this study, we use computer vision and machine learning technology to detect MCTS and estimate their volumes. Fig. 1 and 2 show some examples of 2D monolayer cells, 3D MCTS, and cellular aggregates, which represent MCTS that have failed to form a spherical structure after the addition of cyclo-RGDfK (TPP) [25]. The definition complies with the set of labeled data used to train our ML model in this research. For the purposes of this study, only MCTS were detected. However, our proposed method can be extended and trained to recognize different cellular morphologies having a different specification with a larger set of training data containing all variants of spheroids.

2.1 RELATED WORK

There are many models [5, 27-31] that provide automatic approaches to the identification of cell cultures, compute similar volume estimations for three dimensional objects, or use image detection software. Hou et al. [6] has summarized the existing software for spheroid image analysis, which predominantly focuses on static images generated by high throughput screening. Many of these software require additional non-free supporting software. Some of these approaches are explained below in more detail.

Table 1: Summary of software available for spheroid image analysis [6]

Software	Category	Analysis & visualization	Availability & language
TASI	Time-lapse	Yes	Open source, Matlab
qVISTA	High-throughput	Yes	Software not provided, Matlab
AMIDA, AnaSP	High-throughput	No	Open sourc, Java or Matlab
PCaAnalyser	High-throughput	No	Open source, ImageJ
Phaedra; MetaXpress	High-throughput	No	Commercial
Spheroid Analyzer	Both	No	Open source, ImageJ
SpheroidSizer	Both	No	Open source, Matlab
Celigo; Imaris & Velocity; VTT_Acca	Both	No, No	Commercial

The Celigo cytometer [32] is a functional assay that scans 96-well plates containing spheroids and completes analysis within 10 minutes per plate. Spheroids are identified by image segmentation around the invading cells. the diameter, perimeter and the area of spheroids are measured automatically [32]. Similar software includes Imaris & Velocity and VTT_Acca [33]. However, these analysis techniques are commercial, thereby requiring costly and specialized equipment.

SpheroidSizer [12] is an open-source software that can automatically detect the boundaries of spheroids and perform volume estimation in under 2 seconds per spheroid. However, it only detects one spheroid per image and measures the axial length of a spheroid and requires the non-open source Matlab software. Nevertheless, SpheroidSizer can be extended to detect multiple spheroids in one image, so it should be explored further as a suitable platform for spheroid analysis [12].

Rather than estimating spheroid volume based on a 2D image, the reconstruction of 3D MCTS from 2D projections has been the focus of much research. Volume reconstruction methods exploit a 2D projection of a spheroid to reconstruct its 3D volume using software such as ReViMS, 3-D ImageJ Suite, Amira, and Imaris. ReViMS is an open source tool that automatically segments z-stacks of fluorescence images and estimates the volume of MCTS with a precision and accuracy of greater than 95%. However, it requires the use of a confocal or light sheet fluorescence microscope, which is not always an available resource, and the three-dimensional modeling of each spheroid, which could be problematic for larger data sets [5]. Although ReViMS is suitable for volume estimation, it is not suitable for the goals of this research, which was to achieve both detection and volume estimation using phase contrast imaging, the most commonly used, label-free microscopic method for visualizing cells [34].

Machine learning is becoming an increasingly popular approach for the analysis of medical images. Xue et al. [29] propose a novel framework which integrated CNN with compressed sensing to identify cells to overcome the challenge of cell detection and localization. They take an innovative approach by reframing the problem as a regression task from raw pixels [29]. However, the problem only addresses monolayer cell cultures, so it would be interesting to extend the framework to 3D structures such as spheroids.

Bayramoglu et al. [7] developed an automated method to detect particular cell types present in 3D cultures using a supervised machine learning approach. Similarly, Rasti et al. [8] developed a supervised machine learning approach to detect specific cell types in spheroids using synthetic data, thereby eliminating the need for manual annotation of training nor testing datasets. To the best of our knowledge, a machine learning approach to accomplish spheroid detection and volume estimation has not been undertaken. Thus, we selected our object detection technique, YOLOv2, based on its global reasoning properties and high sensitivity to false positives, which should theoretically allow for the accurate detection of multiple MCTS per image.

YOLO is a one-phase detector [35], which uses a single CNN to simultaneously predict multiple bounding boxes and their corresponding class probabilities. YOLO learns very general representations of objects, resulting in a system which makes more localization errors, but is less likely to predict false positives on a background. Because the state-of-the-art techniques for the creation of spheroids do not strictly produce viable spheroids, the tendency of two-phase models to predict false positives on a background is problematic. Redmon and Farhadi later [36] improved on the YOLO system to address the issue of localization errors by creating YOLOv2. The fully connected layers from the original YOLO were removed and instead anchor boxes were used to predict bounding boxes to increase performance of the network. YOLOv3, outlined by Redmon and Farhadi in 2018 [37], made small incremental improvements to the model which, among other things, improved small object detection. However, this came at the cost of increasing the size of the network. Due to the nature of the spheroid detection problem, where detected spheroids all occupy a similar proportion of the image frame, the trade-off of performance for small-object detection was not desirable. One of our goals for this project was to make it computationally cheap so that it could be used quickly and effectively on non-dedicated systems. YOLO performs better than other state-of-the-art systems in constrained-compute environments [37].

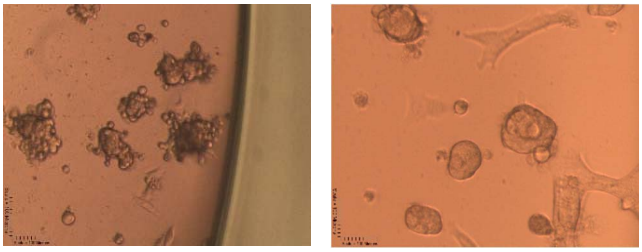

Figure 2. An example of the unaltered spheroid images, used for training and testing.

3 Implementation

3.1 Overview

We propose the use of a deep CNN model based on YOLOv2 to first detect and then recognize spheroids in 10 times magnified images taken by a scope-mounted inverted phase microscope. Fig. 1 and 2 show the varying sizes, clustered cells, visual presentation and the quality of the images, which pose challenges in recognizing the spheroids. We applied multiple strategies to preprocess the images, which is described in this section. However, due to unsatisfactory results we retracted back to using the raw images in our framework to achieve the best results.

The network detects objects and generates bounding boxes around the objects as shown in Fig. 3. Then the objects are classified as spheroids with a generated probability on the certainty of the classification. The dimensions of the bounding boxes are subsequently used in an algorithm to calculate the volumes of the spheroids detected with high

confidence scores. We also explored the potential of an end-to-end framework to pre-process images.

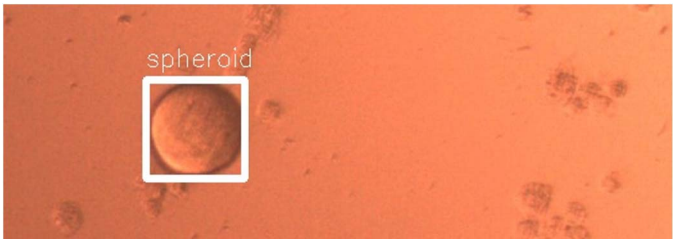

Figure 3. An example of the spheroid detection system with a correctly identified spheroid in a bounding box.

3.2 DATA

The data used for this project was provided by the Myron R. Szewczuk Lab from Queen's University Department of Biomedical and Molecular Sciences, which comprised of 916 manually labelled images. These images were 10 times magnified from the actual cell dimensions. The data set was created by using a scope-mounted inverted phase contrast microscope and contained images of the DU145 prostate carcinoma cell line, which formed prostaspheres under several treatment and control conditions.

For developing the AI deep convolutional network model, we split the data into 65-35% for training and testing respectively. 598 images were used for training and 318 images were used for testing our model.

The images contained at most 10 spheroids per image. The average number of spheroids per image was two. The annotated images contained a scale and were manually annotated. All annotated images were verified by at least one other researcher to ensure accurate labeling. The images had some variance in resolution. The model performed better on higher resolution images.

3.3 IMAGE PRE-PROCESSING

We made several different attempts with the hope of eliminating noise, while still maintaining the key distinctive characteristics of the spheroids. The two most successful methods of image processing are the Canny Edge Detector, and black/white thresholding [39]. Although these methods have been widely used in computer vision, they did not prove to be useful in our study and did not improve the accuracy of spheroid detection. We believe the reason for not seeing any improvement is the highly variable nature of the data set.

The Canny Edge Detection algorithm is a multi-state algorithm which detects a wide range of edges in images [39]. The algorithm first applies a Gaussian filter to smooth noise in images, and then finds the intensity gradient of each image. Next it applies non-maximum suppression and double threshold to determine potential edges, which are finally tracked with hysteresis as shown in Fig. 4.

Thresholding showed the most promising results with a pixel threshold value around 200, where greyscale images have threshold values ranging from 0 (black) to 255 (white). We applied thresholding to images as shown in Fig. 5.

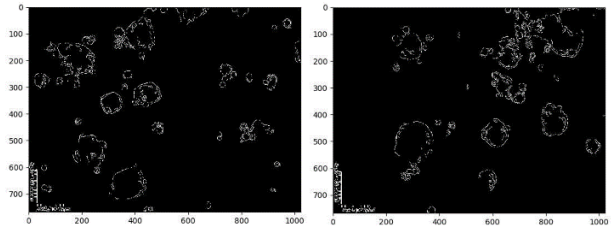

Figure 4. Examples of images that have been processed with the Canny Edge Detection Algorithm.

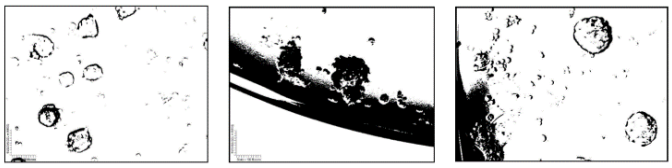

Figure 5. Examples of images that have been processed with SciPy library black and white conversion functionality.

The workflow with the preprocessed images was structured as shown in Fig. 6. The raw image was taken and preprocessed as outlined above. We used the LabelImg software [40] to manually transcribe labels from the manual annotations to the necessary PACAL VOC format for using in our framework. Then the images were reshaped according to the label specifications before being passed into the convolutional neural network for spheroids detection.

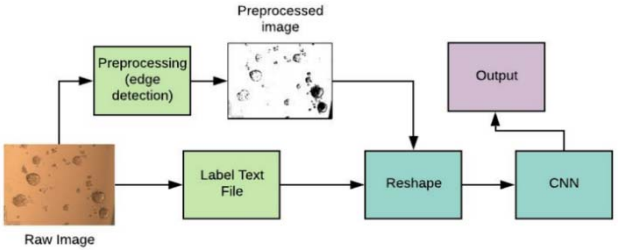

Figure 6. The proposed workflow for integrated data pre-processing.

The preprocessing did not provide a satisfactory accuracy in spheroids detection. The diverse and varying lighting created disparate effects using the SciPy library for images taken on different days. Furthermore, the Canny Edge Detector created unintelligible shapes due to satellites of cells (Fig. 1c) on the periphery of certain spheroids. While certain images worked very well with these two preprocessing methods, in the end, the raw images were deemed to be best suited for training the network and the image preprocessing workflow was abandoned.

3.4 THE CNN MODEL

The custom spheroid detection system was implemented using YOLOv2 with a Darkflow base [35]. Darkflow is a TensorFlow translation of Darknet. Darknet is an open source neural network framework written in C using CUDA for high performance computing purposes. YOLOv2 is the second iteration of the You Only Look Once algorithm originally developed and later extended by Redmon et al. [35-37]. The system is unique in the fact that it treats the problem of object

detection as a single regression problem, utilizing a single convolutional network to simultaneously predict multiple bounding boxes and their corresponding class probabilities [35].

YOLO divides a given image into an S x S grid, with the responsibility of detection falling onto whichever grid cell corresponds to an object's centre. Each grid cell then predicts the possible object bounding boxes and their confidence scores, reflecting how certain the network is in its assertion of a binding, and how accurately it believes in its classification of the object[35]. The Intersection Over Union (IoU) method is used to calculate confidence scores, which takes the area of intersection of the predicted box with the ground truth, divided by the union of the two boxes.

Each bounding box consists of six predictions on a 2D space: the max *x*, the max *y*, the min *x*, the min *y*, the prediction probability, and the classification. In this application, only one-class classification is used to identify if the bounded object is a spheroid or not. To estimate the spheroid volumes, the predictions of the max *x*, the max *y*, the min *x*, and the min *y* are used with the same computational method to manually estimate the spheroids volumes as shown in Eq. 1. The results are compared against the manually annotated spheroids volumes in the labelled data to calculate the accuracy of our approach. In Eq. 1, *a* and *c* represent the average values of width and length respectively.

$$V = \frac{4}{3}\pi a^2 c \qquad \text{Eq. (1)}$$

The network architecture for YOLO is inspired by the GoogLeNet model for image classification [35]. We used the same architecture with 19 convolutional layers and 5 maxpooling layers. The number of channels is doubled after every pooling step and global average pooling is used to make predictions [36]. A breakdown of the network architecture is shown in Fig. 7.

Type	Filters	Size/Stride	Output
Convolutional	32	3×3	224×224
Maxpool		$2 \times 2/2$	112×112
Convolutional	64	3×3	112×112
Maxpool		$2 \times 2/2$	56×56
Convolutional	128	3×3	56×56
Convolutional	64	1×1	56×56
Convolutional	128	3×3	56×56
Maxpool		$2 \times 2/2$	28×28
Convolutional	256	3×3	28×28
Convolutional	128	1×1	28×28
Convolutional	256	3×3	28×28
Maxpool		$2 \times 2/2$	14×14
Convolutional	512	3×3	14×14
Convolutional	256	1×1	14×14
Convolutional	512	3×3	14×14
Convolutional	256	1×1	14×14
Convolutional	512	3×3	14×14
Maxpool		$2 \times 2/2$	7×7
Convolutional	1024	3×3	7×7
Convolutional	512	1×1	7×7
Convolutional	1024	3×3	7×7
Convolutional	512	1×1	7×7
Convolutional	1024	3×3	7×7
Convolutional	1000	1×1	7×7
Avgpool		Global	1000
Softmax			

Figure 7. The Darkflow-19 network architecture showing a breakdown of the filters, the stride, and the output[36].

The layers of the convolutional network are organized in three-dimensions; representing the width, height, and depth of the image. The convolution is performed with the kernels, referred to as filters. The maxpooling layers are used to continuously reduce dimensionality; which in turn helps to diminish the number of parameters and amount of computations in the network, shortens the overall training time and reduces the probability of overfitting. Batch normalization is used to speed up the convergence, stabilize the training, and regularize the model [36]. A linear activation function is used in the final layer, and all other layers use the leaky rectified linear activation function.

3.5 Implementation Environment

We used shared resources from Compute Canada in this research project to implement the prototype framework. Compute Canada's Python virtual environment for Tensorflow was used for implementing the framework and the heterogeneous, general-purpose GPU enabled Graham cluster was used to train the CNN model. The Graham cluster consists of high-performance computing machines with 16 core Intel E5-2683 V4 CPUs running at 2.1 GHz, and with one P100 12g GPU. An additional 100G of RAM was allocated per job to avoid out of memory problems. A total of 30 hours was required to train the CNN model. The weights were saved every 125 steps, allowing testing of the model at different strides and to prevent overfitting. Four different trained models were saved after four different training intervals at iterations (training steps) 5000, 8000, 13625, and 17125, and the best test results were obtained at 13625 steps. The LabelImg software [40] was used for the to manually transcribe labels from manual annotations to the PACAL VOC format for usage with YOLOv2 Darkflow.

4 Results

We measured the accuracy of spheroid detection using precision, recall and F1-score as specified in Eq. 2, 3 and 4 respectively. Our spheroid detection system had a precision of 82.16%, a recall of 71.30% and an F1-score of 76.35%. The system was capable of detecting and measuring spheroids with an accuracy which is comparable to similar applications as discussed in Section 2.1. Rasti et al. compared the average performance of two classifiers to detect a specific cell type in an MCTS culture, which had an average detection accuracy of 68.53% and 94.74% [8]. Unfortunately, the precision, accuracy, and F1-score were not elaborated upon so it is difficult to compare our approach against that of Rasti et al. The leading technique in volume estimation, SpheroidSizer, had a standard deviation of nearly zero when three measurements of 24 spheroids were compared against one another [12]. SpheroidSizer was deemed superior to a manual analysis approach due to lower variability in spheroid measurements [8]. However, the volume estimations were not compared against ground-truth, or manual annotations, as was the case with our approach, so it is difficult to compare the performance of YOLOv2 against SpheroidSizer.

$$precisioin = \frac{true\_positives}{true\_positives + false\_positives} \qquad \text{Eq. (2)}$$

$$recall = \frac{true\_positives}{true\_positives + false\_negatives} \quad \text{Eq. (3)}$$

For each image, a json file was generated as an output containing information about each detected image. The json output as shown below was generated for the image shown in Fig. 3.

4.1 VALIDATION

The 318 test images with bounding boxes and the generated data in the json files were compared against the manual annotations or image labels provided in the data set. We computed the number of spheroids that were correctly identified (true positive), missed (false negative), and falsely identified (false positive). As described before, we saved our model after training it for 5000, 8000, 13625, and 17125 iterations to test the performance using the test images. The results of the ***spheroids classification*** are shown in Fig. 8 below. The best test results were obtained by the model trained for 13625 iterations. The model trained for 17125 iterations was over-trained and provided worse results.

	17125	13625	8000	5000
True Positive	400	410	409	409
False Positive	107	89	91	93
False Negative	175	165	166	166
Precision	78.90%	82.16%	81.80%	81.47%
Recall	69.57%	71.30%	71.13%	71.13%
F1	73.94%	76.35%	76.09%	75.95%

Figure 8. The precision, recall, and F1, at each of the four different steps of training. The best precision, recall, and F1 are highlighted in the colour green, and conversely, the worst are highlighted in red.

The Intersection over Union (IoU) is used to measure the accuracy of spheroid detection. We used Eq. 4 to calculate the IoU using the areas of the ground-truth bounding box from the manually annotated boxes from LabelImg and the predicted bounding boxes from the output of YOLO.

$$IoU = \frac{area\_of\_overlap}{area\_of\_union} \quad \text{Eq. (4)}$$

We performed validation for ***volume calculation*** for the spheroids that were correctly identified. Volumes calculated using Eq. 1 were compared against manually calculated volumes provided in the data set using Eq. 5, where D indicates all correctly detected images.

$$\text{Error} = \sum_D \frac{Abs(actual\ volume - measured\ volume)}{actual\ volume} \quad \text{Eq. (5)}$$

The average IoU achieved in our system was 68.31%, and the average volume prediction accuracy from the successfully identified spheroids was 88.99% for an average error of 11.01%.

5 CONCLUSION AND FUTURE WORK

We attempt to solve the problem of automatic labeling and identification of spheroids using a CNN (Darkflow YOLOv2) and measuring their volume from the dimensions of the bounding boxes. The system is a single-phase image object detector which utilizes a CNN. The network detects objects in the images and predicts bounding boxes around the objects and their class probabilities. The network also outputs images with bound detections, as well as detecting object coordinates and certainty. The data used in our experiments consisted of 916 images of cyclo-RGDfk (TPP) generated spheroids. Several attempts were made at preprocessing the images with Canny Edge Detection and thresholding but ultimately these steps did not improve results. The raw images yielded better results as some key features were lost during the image processing due to uneven lighting and varying resolutions of images. Validations were done by calculating precision, recall and F1-score of the predictions, which yielded 82.16%, 71.30%, and 76.35% respectively. IoU and the volume comparisons were also used to validate the system. To the best of our knowledge, a machine learning approach to accomplish spheroid detection and volume estimation without requiring specialized equipment and software such as Matlab does not exist.

Further work could be done to extend this system to detect a variety of 3D cellular morphologies as not all cell lines form 3D MCTS [19]. For instance, the system could be implemented for the detection and volume estimation of cell aggregates (Fig. 1c), defined as "loose packages of cells" that lack a spherical geometry and may lack cell-cell or cell-extracellular matrix (ECM) interactions [38]. In the context of 3D spheroids generated using cyclo-RGDfK (TPP), PANC-1 pancreatic cancer cells form cellular aggregates as opposed to true spheroids [14]. Unlike measuring spheroids, measuring the size of cell aggregates using a manual approach is challenging due to their non-uniform shape, thereby highlighting the importance of approaches such as YOLOv2 to automate this process. Automating detection and measurement with YOLOv2 using spheroids generated from other cell lines, such as the MDA-MB231 triple negative breast cancer cell line, could be of value as well to compare the performance of YOLOv2 on larger spheroids with less defined borders.

Additionally, data augmentation could be used to greatly increase the quantity of labeled data. Creating additional data is costly and time consuming. Therefore, approaches such as rotation, shifting, creating filters to emulate different light conditions, and introducing luminance distortions similar to the edges of the spheroid sample dishes could be used to improve the training of CNN-based models.

ACKNOWLEDGMENTS

We would like to thank Compute Canada for providing us with the necessary compute resources for this research and our collaborators at Dr. Myron R. Szewczuk's Lab at Queen's University for providing us with the data and helping us with the domain knowledge. We would also like to acknowledge our collaborator Prof. Sergey V Burov at the Synthesis of Peptides and Polymer Microspheres Laboratory in the Institute of Macromolecular Compounds, Russian Academy of Sciences, St Petersburg, Russia for generously providing us the cyclo-RGDfK (TPP) peptide used in the study.

6 REFERENCES

[1] L. C. Kimlin, G. Casagrande, and V. M. Virador, "In vitro three-dimensional (3D) models in cancer research: an update," *Mol Carcinog,* vol. 52, no. 3, pp. 167-82, Mar 2013.

[2] J. M. Kelm and M. Fussenegger, "Microscale tissue engineering using gravity-enforced cell assembly," *Trends Biotechnol,* vol. 22, no. 4, pp. 195-202, Apr 2004.

[3] Y. Fang and R. M. Eglen, "Three-Dimensional Cell Cultures in Drug Discovery and Development," (in eng), *SLAS discovery : advancing life sciences R & D,* vol. 22, no. 5, pp. 456-472, 2017.

[4] F. Piccinini, A. Tesei, C. Arienti, and A. Bevilacqua, "Cancer multicellular spheroids: Volume assessment from a single 2D projection," *Computer Methods and Programs in Biomedicine,* vol. 118, no. 2, pp. 95-106, 2015/02/01/ 2015.

[5] F. Piccinini, A. Tesei, M. Zanoni, and A. Bevilacqua, "ReViMS: Software tool for estimating the volumes of 3-D multicellular spheroids imaged using a light sheet fluorescence microscope," *BioTechniques,* vol. 63, no. 5, pp. 227-229, 2017/11/01 2017.

[6] Y. Hou, J. Konen, D. J. Brat, A. I. Marcus, and L. A. D. Cooper, "TASI: A software tool for spatial-temporal quantification of tumor spheroid dynamics," *Sci Rep,* vol. 8, no. 1, p. 7248, May 8 2018.

[7] N. Bayramoglu *et al.*, "Detection of Tumor Cell Spheroids from Co-cultures Using Phase Contrast Images and Machine Learning Approach," in *2014 22nd International Conference on Pattern Recognition*, 2014, pp. 3345-3350.

[8] P. Rasti, R. Huaman, C. Riviere, and D. Rousseau, "Supervised machine learning for 3D microscopy without manual annotation: application to spheroids", *SPIE Photonics Europe*. SPIE, 2018.

[9] G. Mehta, A. Y. Hsiao, M. Ingram, G. D. Luker, and S. Takayama, "Opportunities and challenges for use of tumor spheroids as models to test drug delivery and efficacy," (in eng), *Journal of controlled release : official journal of the Controlled Release Society,* vol. 164, no. 2, pp. 192-204, 2012.

[10] R. C. Mohs and N. H. Greig, "Drug discovery and development: Role of basic biological research," *Alzheimer's & Dementia: Translational Research & Clinical Interventions,* vol. 3, no. 4, pp. 651-657, 2017/11/01/ 2017.

[11] J. Hoarau-Véchot, A. Rafii, C. Touboul, and J. Pasquier, "Halfway between 2D and Animal Models: Are 3D Cultures the Ideal Tool to Study Cancer-Microenvironment Interactions?," *International journal of molecular sciences,* vol. 19, no. 1, p. 181, 2018.

[12] W. Chen, C. Wong, E. Vosburgh, A. J. Levine, D. J. Foran, and E. Y. Xu, "High-throughput image analysis of tumor spheroids: a user-friendly software application to measure the size of spheroids automatically and accurately," (in eng), *Journal of visualized experiments : JoVE,* no. 89, p. 51639, 2014.

[13] G. Hamilton, "Multicellular spheroids as an in vitro tumor model," *Cancer Letters,* vol. 131, no. 1, pp. 29-34, 1998/09/11/ 1998.

[14] R. Akasov *et al.*, "Sialylation transmogrifies human breast and pancreatic cancer cells into 3D multicellular tumor spheroids using cyclic RGD-peptide induced self-assembly," *Oncotarget,* vol. 7, no. 40, pp. 66119-66134, Oct 4 2016.

[15] X. Li *et al.*, "Functionalized Folic Acid-Conjugated Amphiphilic Alternating Copolymer Actively Targets 3D Multicellular Tumour Spheroids and Delivers the Hydrophobic Drug to the Inner Core," *Nanomaterials (Basel, Switzerland),* vol. 8, no. 8, p. 588, 2018.

[16] X. Cui, Y. Hartanto, and H. Zhang, "Advances in multicellular spheroids formation," *J R Soc Interface,* vol. 14, no. 127, Feb 2017.

[17] D. Khaitan, S. Chandna, M. B. Arya, and B. S. Dwarakanath, "Establishment and characterization of multicellular spheroids from a human glioma cell line; Implications for tumor therapy," *J Transl Med,* vol. 4, p. 12, Mar 2 2006.

[18] D. Khaitan and B. S. Dwarakanath, "Multicellular spheroids as an in vitro model in experimental oncology: applications in translational medicine," *Expert Opin Drug Discov,* vol. 1, no. 7, pp. 663-75, 2006.

[19] C. R. Thoma, M. Zimmermann, I. Agarkova, J. M. Kelm, and W. Krek, "3D cell culture systems modeling tumor growth determinants in cancer target discovery," *Adv Drug Deliv Rev,* vol. 69-70, pp. 29-41, Apr 2014.

[20] F. Hirschhaeuser, H. Menne, C. Dittfeld, J. West, W. Mueller-Klieser, and L. A. Kunz-Schughart, "Multicellular tumor spheroids: An underestimated tool is catching up again," *Journal of Biotechnology,* vol. 148, no. 1, pp. 3-15, 2010/07/01/ 2010.

[21] R. Edmondson, J. J. Broglie, A. F. Adcock, and L. Yang, "Three-dimensional cell culture systems and their applications in drug discovery and cell-based biosensors," (in eng), *Assay and drug development technologies,* vol. 12, no. 4, pp. 207-218, 2014.

[22] T.-M. Achilli, J. Meyer, and J. R. Morgan, "Advances in the formation, use and understanding of multi-cellular spheroids," (in eng), *Expert opinion on biological therapy,* vol. 12, no. 10, pp. 1347-1360, 2012.

[23] A. S. Nunes, A. S. Barros, E. C. Costa, A. F. Moreira, and I. J. Correia, "3D tumor spheroids as in vitro models to mimic in vivo human solid tumors resistance to therapeutic drugs," *Biotechnol Bioeng,* Oct 27 2018.

[24] A. S. Nunes, E. C. Costa, A. S. Barros, D. de Melo-Diogo, and I. J. Correia, "Establishment of 2D Cell Cultures Derived From 3D MCF-7 Spheroids Displaying a Doxorubicin Resistant Profile," *Biotechnol J,* p. e1800268, Sep 22 2018.

[25] R. Akasov *et al.*, "Formation of multicellular tumor spheroids induced by cyclic RGD-peptides and use for anticancer drug testing in vitro," *Int J Pharm,* vol. 506, no. 1-2, pp. 148-57, Jun 15 2016.

[26] A. P. Mould *et al.*, "Defining the topology of integrin alpha5beta1-fibronectin interactions using inhibitory anti-alpha5 and anti-beta1 monoclonal antibodies. Evidence that the synergy sequence of fibronectin is recognized by the amino-terminal repeats of the alpha5 subunit," *J Biol Chem,* vol. 272, no. 28, pp. 17283-92, Jul 11 1997.

[27] Z. Krawczyk, Starzynski, J, "Bones Detection in the Pelvic Area on the Basis of YOLO Neural Network," presented at the IEE 19th International Conference Computational Problems of Electrical Engineering, Banska Stiavnica, Slovakia 9-12 September, 2018.

[28] R.-Z. Lin, L.-F. Chou, C.-C. M. Chien, and H.-Y. Chang, "Dynamic analysis of hepatoma spheroid formation: roles of E-cadherin and β1-integrin," *Cell and Tissue Research,* vol. 324, no. 3, pp. 411-422, 2006/06/01 2006.

[29] Y. Xue, N. Ray, J. Hugh, and G. Bigras, "A novel framework to integrate convolutional neural network with compressed sensing for cell detection," in *2017 IEEE International Conference on Image Processing (ICIP)*, 2017, pp. 2319-2323.

[30] C. M. Garvey *et al.*, "A high-content image-based method for quantitatively studying context-dependent cell population dynamics," *Sci Rep,* vol. 6, p. 29752, Jul 25 2016.

[31] L. Hou, Nguyen, V, Samaras, D, Kurc TM, Gao, Y, Zhao, T, Saltz, JH, , "Sparse Autoencoder for Unsupervised Nucleus Detection and Representation in Histopathology Images," *arXiv e-prints,* 2017.

[32] M. Vinci *et al.*, "Advances in establishment and analysis of three-dimensional tumor spheroid-based functional assays for target validation and drug evaluation," (in eng), *BMC biology,* vol. 10, pp. 29-29, 2012.

[33] V. Harma *et al.*, "Lysophosphatidic acid and sphingosine-1-phosphate promote morphogenesis and block invasion of prostate cancer cells in three-dimensional organotypic models," *Oncogene,* vol. 31, no. 16, pp. 2075-89, Apr 19 2012.

[34] M. Kaakinen, S. Huttunen, L. Paavolainen, V. MarjomÄKi, J. HeikkilÄ, and L. Eklund, "Automatic detection and analysis of cell motility in phase-contrast time-lapse images using a combination of maximally stable extremal regions and Kalman filter approaches," *Journal of Microscopy,* vol. 253, no. 1, pp. 65-78, 2014/01/01 2014.

[35] J. Redmon, S. Divvala, R. Girshick, and A. Farhadi, "You Only Look Once: Unified, Real-Time Object Detection," *arXiv e-prints,* Accessed on: June 01, 2015Available: https://ui.adsabs.harvard.edu/\#abs/2015arXiv150602640R

[36] J. Redmon, Farhadi, A., "YOLO9000: Better, Faster, Stronger," presented at the IEEE Computer Society Conference on Computer Vision and Pattern Recognition, Honolulu, Hawaii, 2017.

[37] J. Redmon and A. Farhadi, "YOLOv3: An Incremental Improvement," *arXiv e-prints,* Accessed on: April 01, 2018Available: https://ui.adsabs.harvard.edu/\#abs/2018arXiv180402767R

[38] L.-B. Weiswald, D. Bellet, and V. Dangles-Marie, "Spherical Cancer Models in Tumor Biology()," *Neoplasia (New York, N.Y.),* vol. 17, no. 1, pp. 1-15, 01/23

[39] L. Ding and A Goshtashy, 2001. *On the Canny Edge Detector*. Pattern Recognition. Vol. 34, Issue 3, Pages 721-725.

[40] B.Russel, A. Torralba, And W. T. Freeman. 2013, *LabelImg* MIT, Computer Science and Artificial Intelligence Laboratory.